Polymer Chemistry

RSCPublishing

Article

Enzymatic Synthesis of Hyaluronic Acid Vinyl Esters for Two-photon Microfabrication of Biocompatible and Biodegradable Hydrogel Constructs

Cite this: DOI: 10.1039/x0xx00000x

Received 00th January 2014,
Accepted 00th January 2014

DOI: 10.1039/x0xx00000x

www.rsc.org/

Xiao-Hua Qin,[a] Peter Gruber,[b] Marica Markovic,[b] Birgit Plochberger,[c] Enrico Klotzsch,[c+] Jürgen Stampfl,[b] Aleksandr Ovsianikov,[b] and Robert Liska*[a]

Two-photon polymerization (2PP) allows 3D microfabrication of biomaterial scaffolds with user-defined geometry. This technique is highly promising for 3D cell culture and tissue engineering. However, biological applications of 2PP require photopolymerizable hydrogels with high reactivity and low cytotoxicity. This paper describes a novel hydrogel system based on hyaluronic acid vinyl esters (**HA-VE**), which enabled fast 2PP-fabrication of 3D hydrogel constructs with μm-scale accuracy. A series of **HA-VE** macromers with tunable degrees of substitution were synthesized by lipase-catalyzed transesterification. **HA-VE** gels were proved to be injectable, photocurable, enzymatically degradable and mechanically comparable to various soft tissues. Owing to the unique molecular design, degradation products of **HA-VE** gels through hydrolysis are non-toxic polyvinyl alcohol and adipic acid. Furthermore, **HA-VE** gels were systematically characterized and compared to HA-acrylates (**HA-AC**) and HA-methacrylates (**HA-MA**) gels including macromer cytotoxicity, photoreactivity, swelling, and gel stiffness. Cytotoxicity assay with L929 fibroblasts revealed that **HA-VE** was significantly less toxic than **HA-AC** ($P<0.01$) and **HA-MA** ($P<0.05$). Crosslinking efficiency of **HA-VE** was comparable to HA-AC and much higher than **HA-MA**. Although the reactivity of **HA-VE** for homopolymerization was insufficient for 2PP, it was demonstrated that thiol-ene chemistry could substantially improve its reactivity. This optimization led to 2PP-fabrication of a **HA-VE** hydrogel construct with μm-scale accuracy. Low cytotoxicity, high reactivity and good biodegradability makes **HA-VE** promising candidates for biological applications in cell culture and tissue engineering.

Introduction

Covalently crosslinked hydrogels have been widely used for various biomedical applications including but not limited to three-dimensional (3D) cell culture, wound healing, and tissue regeneration.[1-3] To recapitulate the extracellular matrix (ECM) of human tissues, development of ECM-mimetic hydrogels with highly controlled architectures is increasingly important.[4] It is well established that cellular proliferation, migration, differentiation and tissue regeneration are largely dependent on the matrix properties,[5, 6] such as ligand density,[7] stiffness,[8] and geometry.[9] A variety of fabrication techniques are extensively sought to engineer 3D hydrogel constructs with controlled geometry to provide tissue-specific biological functions.[10, 11] Photolithography is a suitable approach for fabrication of sophisticated hydrogel structures with spatiotemporal control of photochemical events.[12-14] For instance, Tsang et al. utilized single-photon lithography to fabricate hydrogel constructs as artificial hepatic tissues.[15] It is noteworthy that this method is based on iterative photo-crosslinking of polyethyleneglycol diacrylates (PEGDA) using three different photo-masks. Though complex gel structures can be formed, this process requires laborious manipulation of the removable spacers, thus the feature size being intrinsically limited by the spacer thickness. The resolution reported in this study was around 300 μm,[15] which is one order of magnitude larger than the size of most mammalian cells and two to three orders of magnitude above the size that needs to be controlled to efficiently influence cell fate.[16]

As there is increasing knowledge on cell-ECM interactions,[16, 17] it is increasingly important to engineer biomimetic hydrogels with (sub)cellular-scale features due to the fact that cells sense and respond to their 3D environment at the (sub)micron-scale.[6] Among various engineering approaches,[18] two-photon lithography has presented the most promise to precisely engineer 3D hydrogels.[19, 20] For instance, previous work by Anseth and co-workers has established the concept of photodegradable hydrogels where hydrogel niches can be accurately probed in 3D via two-photon-induced degradation.[21] On the opposite side of degradation, two-

photon polymerization (2PP) allows fabrication of 3D hydrogel constructs with user-defined architectures while keeping the μm-scale geometrical control.[22] The principle in 2PP is that two-photon-excited chemical processes (i.e., radical formation and polymerization) are highly localized in a 1 μm^3-scale volume focused by a near-IR laser beam. Though a few successes reported,[22] biological translation of 2PP technique into tissue engineering applications is currently challenged by the shortage of photopolymerizable soft materials that are highly reactive while low cytotoxic. Different from conventional single-photon lithography, macromers used in 2PP should possess a much higher reactivity since 2PP process is based on simultaneous absorption of two photons by one photoinitiator (PI), which occurs only in the most focused area with low probability.[19, 23] Therefore, most reports on the 2PP processing of hydrogels utilized synthetic polymers with highly reactive acrylate groups such as PEGDA.[22]

While PEGDA has been extensively used for photolithographic manufacturing of 3D hydrogels,[15, 24] it is noteworthy that toxic effects and long-term clinical safety of residual macromers and/or acrylate groups has aroused significant concern.[25] On one hand, acrylated monomers are prone to induce inflammatory responses, presumably due to Michael-addition reactions with amine groups of human tissues. On the other hand, as a result of high reactivity, degradation of polyacrylates often generate high MW polyacrylic acids [Supporting Information (SI), Table S1] which are difficult to be excreted from human body and prone to cause local inflammation due to the high number of acidic groups. Toxicity issue of acrylate chemistry led us to develop alternative less cytotoxic photopolymers for lithography-based soft tissue engineering. To minimize toxicity, we turned our attention to vinyl esters (VEs) owing to the following reasons: first, our previous work proved that cytotoxicity of VEs on osteoblasts was at least two orders of magnitude lower than that of acrylates analogues;[26] second, major degradation products of polyVEs are low MW polyvinyl alcohol (PVA) which is FDA-approved biocompatible polymer; third, the moderate reactivity of VEs could be greatly improved using thiol-ene chemistry.[27] Furthermore, seminal work by Anseth and co-workers has demonstrated that hydrogel systems based on photoinitiated thiol-norbornene reactions provide fast kinetics, spatiotemporal control and cytocompatible reaction conditions.[28, 29] These efforts motivated us to explore thiol-VE reactions for 2PP microfabrication of hydrogels. We have recently reported the first hydrogel precursor with pendant VE groups (gelatin VE, GH-VE) and its copolymerization with free cysteines donated by reduced albumin.[30] Although arbitrary hydrogel structures were produced by 2PP, reactivity of GH-VE was relatively low because the number of VE groups (~3 per chain) was intrinsically limited by the number of lysine residues.

In the search for a substrate with more reaction sites, we turned our attention to a major ECM component-hyaluronan (HA). HA is a linear biopolymer ubiquitously distributed in the ECM of many connective tissues.[31] Given the biocompatibility of HA, researchers have utilized a wide variety of HA derivatives for different tissue engineering applications,[31] including oxidizable thiolated HA,[32] in-situ clickable HA derivatives,[33, 34] and photocrosslinkable (meth)acrylated HA.[35-37] However, to our best knowledge, hydrogels based on HA vinyl esters (**HA-VE**) remains unexplored in the fields of biomaterials and tissue engineering.

Here, we report the synthesis and characterization of **HA-VE** macromers and laser fabrication of a 3D hydrogel construct of **HA-VE** by two-photon lithography. Specifically, **HA-VE** macromers with tunable degree of substitution (DS) are synthesized using lipase-catalyzed transesterification reactions between hydroxyl groups in HA and divinyl adipate (DVA, Scheme 1). It is hypothesized that: 1) **HA-VE** with tunable DS could be prepared by tuning the reaction time and stoichiometry between DVA and HA; 2) these macromers would provide hydrogels with tunable properties (reactivity, crosslinking density and gel modulus); 3) the use of thiol-ene chemistry may increase the reactivity of **HA-VE** to a sufficient level for 2PP. Furthermore, we are interested in comparing **HA-VE** with (meth)acrylated HA with a focus on cytotoxicity, and photo-reactivity. Finally, we explore 3D microfabrication of a **HA-VE** hydrogel construct using two-photon lithography.

Scheme 1. Reaction scheme for the synthesis of HA vinyl esters (**HA-VE**)

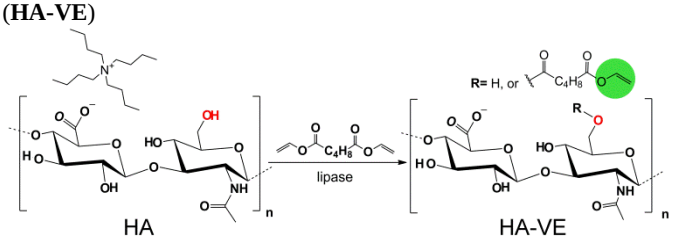

Results and Discussion

Synthesis. In this study, low MW HA (11.4 kDa, PDI:~1.6) was prepared through acidic degradation of commercial high MW HA (1.3 MDa) and used as the substrate.[44] In order to synthesize **HA-VE**, lipase-catalyzed transesterification was selected as the synthetic strategy (Scheme 1). Primary hydroxyl groups of HA were reacted with excessive DVA under the catalysis of lipase (CAL-B). Although similar lipase-catalyzed reactions have been explored in literature,[45, 46] most work focused on the functionalization of di-saccharides or tri-saccharides with polymerizable moieties. It is accepted that the choice of solvent plays an important role in determing the reaction efficiency. On one hand, the solvent should render the substrates soluble and provide a homogeneous reaction media; on the other hand, the solvent should be benign to keep the activity of lipases. For example, Lin et al. proved that a mixture of acetone and ionic liquids was an ideal solvent pair for lipase-catalyzed reactions.[46] We initially attempted to use such a solvent system to functionalize HA with DVA moieties. However, no substitution was observed presumably due to the limited solubility of HA.

In the search for a method that permits HA dissolution while being lipase-friendly, we turned our attention to a two-step approach. First, sodium salt of HA was exchanged with bulky quaternary ammonium cation (tetrabutylammonium, TBA) to form HA-TBA, which is more hydrophobic and thus soluble in DMSO. Second, dissolved HA-TBA was reacted with 3-fold excess of DVA under the catalysis of CAL-B. Notably, the side product of this reaction was merely acetaldehyde (b.p, 20.7 °C) that can be easily removed. (continued)

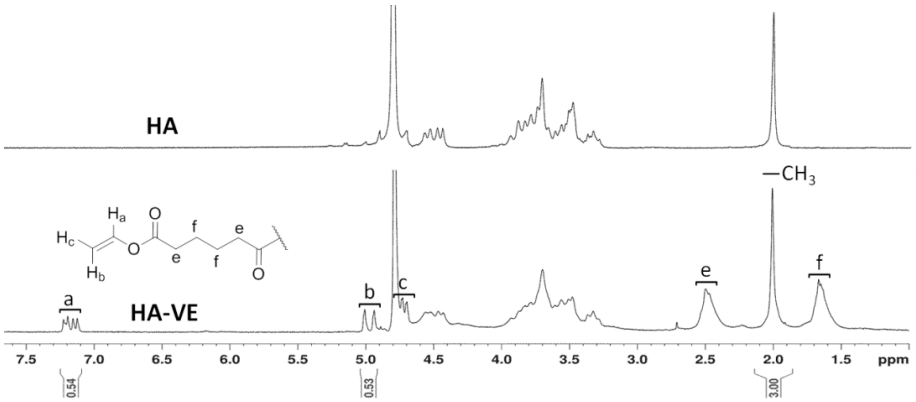

Figure 1 ^{1}H-NMR (D_2O) spectra of **HA** and **HA-VE.**

After reaction, the products were purified by general liquid-liquid extraction and subsequent dialysis against NaCl. Although the incorporation of DVA moieties may increase the substrate hydrophobicity, it was found that the **HA-VE** products retained good water-solubility (max. ~ 30 wt%).

To evaluate the synthesis, comparative NMR spectra (HA vs. **HA-VE**) were measured in D_2O. In comparison with HA, the spectrum of **HA-VE** (Figure 1) showed new peaks at 1.7 (f), 2.52 (e), 4.80-5.03 (b, c) and 7.20 (a) ppm that correlate with the proton signals of DVA (SI, Figure S5). Importantly, the integration of methyl protons of HA at 2.01 ppm can be utilized as reference for the determination of DS by calculating its relative ratio to that of the unsaturated proton (a) at 7.20 ppm. To further confirm the success of synthesis, comparative ATR-FTIR spectra (i.e., HA, DVA and **HA-VE**) were measured (Fig. S1). IR-spectrum of **HA-VE** showed characteristic signals of DVA at 1735 cm^{-1} (C=O), and 1640 cm^{-1} (C=C) in comparison with that of HA. Together, these results proved that the synthesis of **HA-VE** was successful.

To test the feasibility of **HA-VE** with tunable DS, we investigated the influence of reaction time and reactants stoichiometry on DS (Table S2). As the reaction time increased from 24 h to 72 h (Entry 1-3), the DS increased from 0.13 to 0.34. On the other hand, as the stoichiometry increased from 1:1 to 3:1 (Entry 1-6), the DS was raised in varying degree from 0.33 to 1.04. When the reaction time was prolonged to 96 h (Entry 7), the DS value as high as 1.25 was obtained. This value exceeded 1.0 presumably due to the contribution of the secondary hydroxyl groups, which are supposed to be less reactive than primary ones.

Photolymerization of HA-VE. To prove that **HA-VE** is polymerizable, **HA-VE** gel pellets were firstly prepared by UV-photopolymerization in a PDMS mold. I2959 was selected as single-photon initiator due to its good water-solubility and biocompatibility.[47, 48] It is assumed that hydrogel networks could be formed through radical-mediated homopolymerization of VE groups and subsequent intermolecular crosslinking (Figure 2, top). After photocrosslinking, the **HA-VE** gels were slightly yellow but transparent (Figure 2, right-bottom). This is consistent with the appearance of another VE-based hydrogel (GH-VE) as described in our previous work.[30]

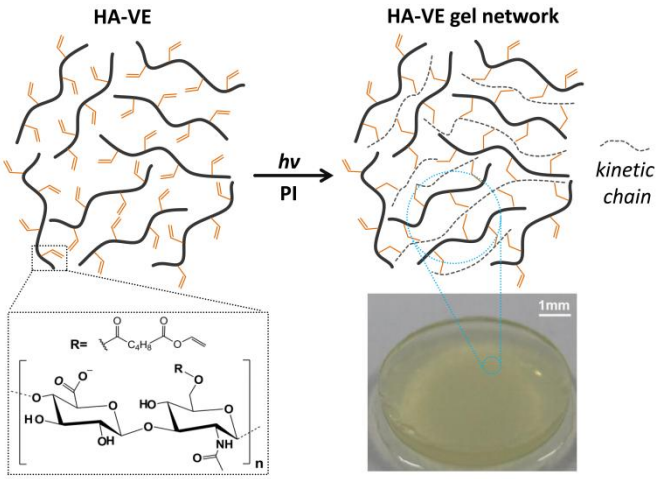

Figure 2 Schematic showing the hydrogel formation by photopolymerization and a captured image of **HA-VE** gel pellet.

Influence of DS on Photoreactivity. Photoreactivity of hydrogel precursors plays an important role in determining the access to 2PP microfabrication.[22] To quantify the photoreactivity and crosslinking efficiency of **HA-VE**, we selected *in-situ* photo-rheometry where UV-Vis light (320-500 nm) is integrated to a plate-to-plate rheometer in the oscillatory mode (SI, Figure S2). This method has proven to be a versatile approach for real-time characterization of gel formation kinetics and bulk mechanical properties.[28, 30] While the exact initiating mechanism in 2PP is not fully understood yet,[19] we hypothesize that single-photon rheometry studies would help pre-evaluate the reactivity of gel precursors prior to 2PP trials.

To test the hypothesis that macromer DS could influence gel physicochemical properties, **HA-VE**s with three different DS (0.13, 0.21, and 0.54) were screened using photo-rheometry at 10% macromer content and 0.5% I2959 concentration in PBS. As shown in Figure 3a, the elastic moduli (G´) of **HA-VE** gels were monitored as a function of UV irradiation time (from 60 s) till a G´-plateau was observed. As the increase of DS from 0.13, 0.21 to 0.54 (SI, Table S3), G´ was gradually shifted from 11.5 kPa and 23.2 kPa to 36.4 kPa, indicating the increase of network crosslinking density. Furthermore, gel points are defined in the vicinity of the elastic and viscous moduli crossover (G´´) as described elsewhere.[49] (continued)

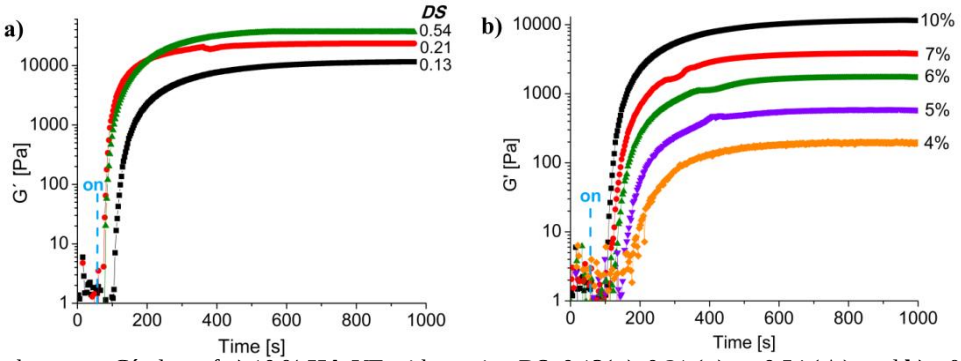

Figure 3 Photo-rheometry G´-plots of **a)** 10 % **HA-VE** with varying DS: 0.13(■), 0.21 (●), or 0.54 (▲); and **b)** x % **HA-VE** (DS-0.13) with varying macromer contents (x=10, 7, 6, 5, 4); 0.5 % I2959, 15 mW cm^2.

It was found that the gel point was shortened from 95 s and 20 s to 16 s, showing that photoreactivity was improved owing to the increase of VE group concentration. Together, these results suggest that by tuning the DS it is feasible to finely control both photoreactivity and physical properties of **HA-VE** gels.

Influence of Macromer Content. To prove that mechanical properties of **HA-VE** gels are physiologically-relevant and comparable to varying soft tissues,[50] we investigated the influence of macromer (**HA-VE**, DS=0.13) concentration on G´-plateau values (Figure 3b). It was found that for 4-10 % **HA-VE** gels, the G´-plateau values were located in a broad range from 200 Pa to 12 kPa (SI, Table S4). Meanwhile, as the macromer content decreased from 10 % to 4 %, the gel point was prolonged from 45 s to 123 s gradually, indicating the influence on photoreactivity.

Temporal Control. An unique advantage of photocurable hydrogel systems is that macromer solutions can be injected into an prescribed area in a minimally invasive surgery and the subsequent curing process can be precisely controlled with light.[14] To prove that the formation of **HA-VE** gels is exclusively due to light exposure (i.e., under temporal control), another photo-rheometry measurement of **HA-VE** was performed. To observe the temporal effects, the UV-light was switched off for 80s at 100s and again at 260s during the measurement (
Figure 4). Without light exposure, negligible modulus change was evidenced by the horizontal plots in the ´´off´´ regions.

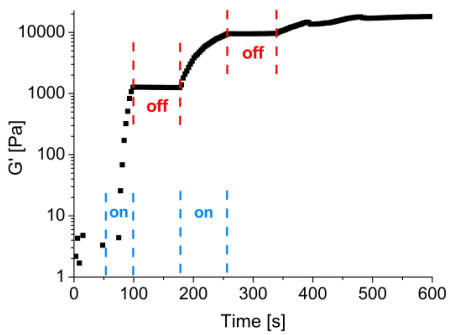

Figure 4 A case photo-rheometry study showing the temporal control on gel formation. (10 % **HA-VE**, DS=0.13; 0.5 % I2959, 15 mW cm^2)

Enzymatic Degradation. Another design criterion for a hydrogel system is the ability to be biodegradable (either by enzyme or by hydrolysis), which is an important feature for tissue remodeling.[6]

Based on an adapted protocol by Fairbanks et al.,[28] *in-situ* rheometry was applied to monitor the enzymatic degradation process (Figure 5) of **HA-VE** gels upon exposure to varying amount of hyaluronidase (Hase). Both the elastic moduli (G´) and loss modulus (G´´) could be monitored in real time within the degradation process (Figure 5a). It was found that all the G´ decreased gradually owing to the biochemical response of **HA-VE** to Hase, which can be explained as the cleavage of linkages between HA units by Hase. Furthermore, it was found that the degradation rate was dependent on the enzyme dose (Figure 5b). It is supposed that the modulus decrease by hydrolytic degradation was not significant during the measurement (~10 h). Given a longer time scale, however, it is hypothesized that **HA-VE** gels are also hydrolytically degradable. We previously studied the *in-vitro* degradation process of polyVEs in comparison with polylactide (PLA) and poly(meth)acrylates.[26] The degradation rate of polyVEs was ~2 times lower than that of PLA and much higher (>10 times) than that of poly(meth)acrylates.

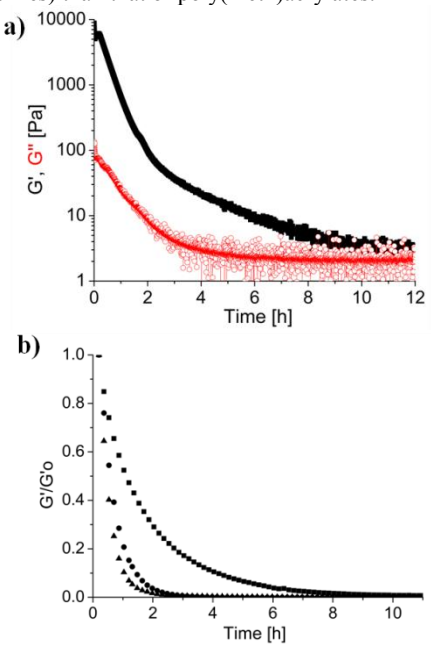

Figure 5 *In-situ* monitoring the degradation process of **HA-VE** gels using rheometry: **a)** a case example showing the gel moduli (G´, G´´) decline due to enzymatic degradation; **b)** normalized G´-plots of 10 % **HA-VE** gels exposed to varying amounts of Hase: 10 (■), 30 (●), or 60 (▲) mg/mL. (G´$_0$: initial G´)

Together, the degradation pathways of **HA-VE** gels are proposed (Figure 6). The degradation products should be PVA, adipic acid and **HA** fragments. It is noteworthy that the toxicity of adipic acid is as low as that of citric acid.[51] The analysis thus leads to a conclusion that **HA-VE** gels are fully biodegradable and generate non-toxic degradation products, making it extremely promising for potential biomedical applications. However, we confess that it is challenging to compare *in-vitro* and *in-vivo* situations. Further investigation into the degradation kinetics of **HA-VE** gels under physiological conditions is warranted for potential clinical applications.

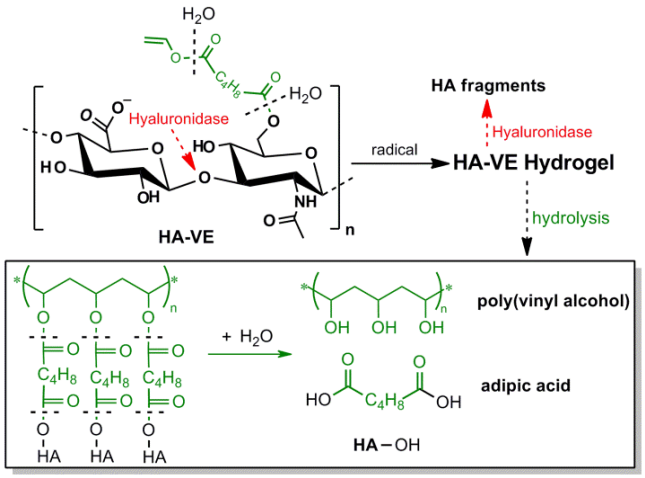

Figure 6 Proposed degradation mechanisms of **HA-VE** hydrogels.

Comparative Analysis of HA Derivatives. In order to compare **HA-VE** with its (meth)acrylates analogs (Figure 7a), we used a **HA-VE** macromer (DS=0.54) and compared it to acrylated HA (**HA-AC**, DS=0.49) and methacrylated HA (**HA-MA**, DS=0.57). Both reference macromers were synthesized as previously reported,[38,39] except using the same substrate as for **HA-VE**.

Cytotoxicity. Cytotoxicity of three macromers on L929 mouse fibroblasts were evaluated using Presto-Blue assay. We initially studied the toxic effects of HA substrate at three concentrations (10 %, 1 % and 0.1 %, SI, Figure S3). Surprisingly, it was found a 10 % **HA** solution induced a significant decrease of cell metabolic activity. This can be attributed to the interaction between **HA** and CD44 receptors on L929 cells. A similar phenomenon has been reported in a recent study where metabolic activity of NIH-3T3 fibroblast was depressed due to the presence of **HA**.[52] Hence, we chose 1 % and 0.1 % as working concentration in further toxicity measurements. As shown in Figure 7b, the toxicity of **HA-VE** solution (1 %) was significantly lower than that of **HA-AC** ($P<0.01$) and that of **HA-MA** ($P<0.05$). When the macromer solutions were diluted to 0.1%, no significant differences between the four samples could be observed.

Photoreactivity. We next analyzed the reactivity difference of three macromers using photo-rheometry. To quantitatively evaluate the reactivity, we focused on two important parameters of photopolymers: 1) slope value of the plotted G´-curves and 2) induction time. As shown in Figure 7c, slope values indicate the respective reactivity follows this order: **HA-AC>>HA-VE>HA-MA**. Notably, homopolymerization rate of **HA-VE** was at least three times lower when compared to **HA-AC**. The reactivity difference can also be evidenced by the differences in induction time where the onset time of **HA-VE** or **HA-MA** was nearly the twice relative to that of **HA-AC**. We next tested the lower macromer content limit of **HA-AC**, **HA-MA**, and **HA-VE** to form a gel upon a 15 min UV exposure. Both **HA-AC** and **HA-VE** form gels as low as 2.5 % whereas the lower limit of **HA-MA** was 5 %, indicating the lower crosslinking efficiency.

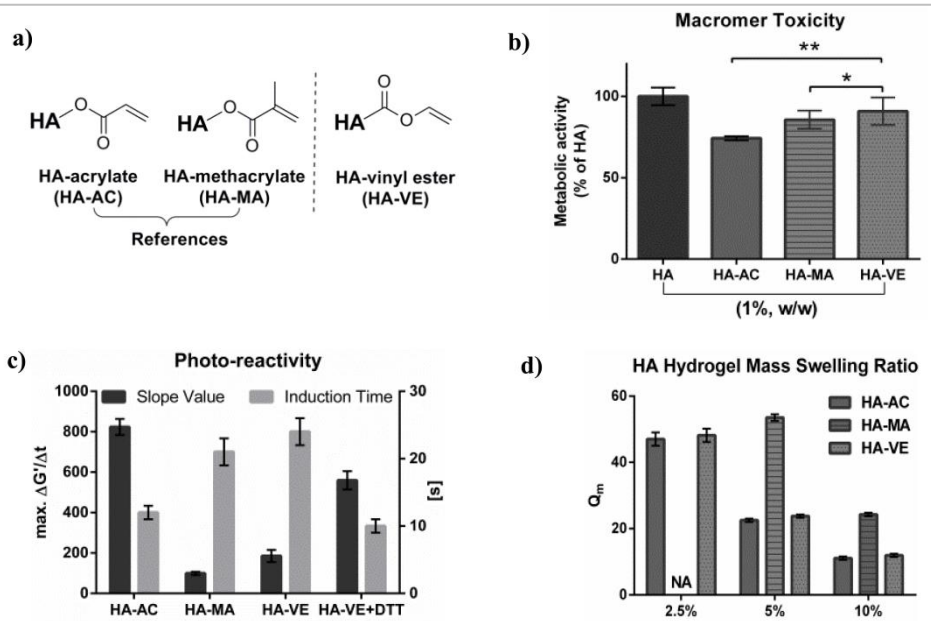

Figure 7 Comparative characterization of **HA-AC**, **HA-MA** and **HA-VE**. **a)** Chemical structures of (meth)acrylate and vinyl ester groups; **b)** Cytotoxicity: metabolic activity of L929 cells after 24 h incubation with four macromer solutions (1 %), *P<0.05,**P<0.01; **c)** Photoreactivity: slope values (black) and induction time (grey) of G´-plots of four HA gel formulations (10%); and **d)** Swelling: equilibrium mass swelling ratio **(Q_m)** of HA gels formed at varying macromer contents (2.5 %, 5 %, 10 %), NA: not applicable.

Swelling Ratio. Swelling behavior is a characteristic feature of hydrogels and important for one to target a specific application.[4] The swelling ratio can give a good indication of the network structure: i.e., the higher swelling ratio, the looser gel network. We screened the equilibrium mass swelling ratio of **HA-AC**, **HA-MA**, and **HA-VE** gels with varying macromer contents (Figure 7d). Equilibrium mass swelling ratio ($\mathbf{Q_m}$) of **HA-VE** gels was around 45 (2.5 %), 20 (5 %) and 10 (10 %), respectively. These values are comparable to those of **HA-AC** gels, showing similar network structures and final macromer conversion. In comparison, **HA-MA** gels present much higher $\mathbf{Q_m}$ values of 50 (5 %) and 25 (10 %). Together, the observed differences in $\mathbf{Q_m}$ values not only reflects the varying network structures, but in turn implies the influences of macromer reactivity and crosslinking efficiency.

Gel Young's Modulus. Given that rheometry is limited to measure gel modulus at the bulk scale whereas cells respond to local forces at the micro- and nanoscale level,[53] we measured the Young's modulus of **HA** gels by nanoindentation using atomic force microscopy (AFM). Prior to AFM test, hydrogel samples were UV-polymerized on top of methacrylated glass slides and then soaked in H_2O for 24 h. Since **HA-MA** gels formed at 5% were too sticky to be measured, hydrogel samples were measured at 10% macromer content. Comparison of Young's modulus values (Figure 8) suggests a gel elasticity order: **HA-AC>HA-VE>HA-MA**, which is consistent with the swelling ratio values (Figure 7d). Interestingly, the network density difference of **HA-AC** and **HA-VE** gels is less significant than the reactivity difference of corresponding macromers. This is attributed to the unique polymerization kinetics of VEs which was previously demonstrated by Heller et al.[26]: i.e., VEs undergo homopolymerization at a much lower rate relative to that of acrylates analogs but finally achieve a comparable conversion.

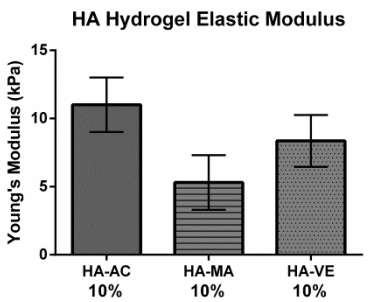

Figure 8 Young's modulus values of **HA** gels formed at 10% macromer content.

Reactivity Optimization. With these results in mind, we attempted 2PP microfabrication of **HA-VE** gels (10%) using an efficient two-photon initiator (2.2 mM P2CK, SI, Figure S4).[42] However, the initial structuring did not succeed even at the maximum laser dosage (> 200 mW). This should be addressed to the limited reactivity of **HA-VE** towards homopolymerization. To improve the reactivity, we turned to thiol-ene chemistry where efficient chain-transfer reactions may be utilized (Figure 9).[54] By using photo-rheometry, we analyzed the influence of a model compound (dithiothreitol, DTT) on the gelation kinetics of **HA-VE**. It was found that addition of appropriate amount of DTT (n_{-SH}:n_{-ene}=0.2-1) can drastically improve the reactivity of **HA-VE** and shorten the plateau time (n_{-SH}:n_{-ene}=0.4, Figure 9). Though reactivity increased, a decline of G´-plateau value was also observed when the thiol to ene ratio exceeds a certain value (~0.6), which is consistent with previous observations related to thiol-ene networks.[54] To maintain the gel modulus, an optimal **HA-VE**/DTT formulation (n_{-SH}:n_{-ene}=0.4) was selected. To prove whether this formulation is comparable to **HA-AC**, further analysis (Figure 7c) showed that the slope value increased from 180 to 570 (800 for **HA-AC**) while the induction time was shortened from 24 s to 9 s (11 s for **HA-AC**). It has to be noted that the thiol-ene chemistry gives no advantages for increasing the polymerization rate of acrylates. And even in the case of methacrylates, addition of thiols slows down the polymerization dramatically.[54]

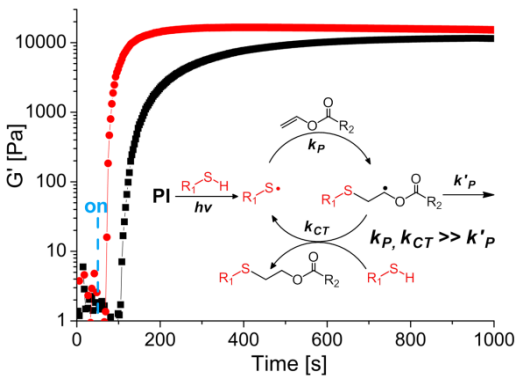

Figure 9 Photo-rheometry study of 10% **HA-VE** (■) and 10% **HA-VE**/DTT (●, n_{-SH}:n_{-ene}=0.4) and proposed mechanism of thiol-VE photopolymerizations (PI: photoinitiator).

Although the reactivity of HA-VE was substantially improved, it is unclear that whether the use of DTT would induce potential cytotoxic effects. Therefore, we tested the cytotoxicity of DTT using Presto Blue assay. Surprisingly, we found that it is not toxic at high concentrations (>2 mM), yet toxic at lower concentrations (<1 mM). These results are consistent with a previous study related to the cytotoxicity of DTT.[55] We argue that the reductive nature of DTT might undermine the reliability of Presto Blue assay which is based on the reduction of Presto Blue reagent by the cytosol of viable cells. Nevertheless, DTT has been recently used for *in situ* photoencapsulation of pancreatic cells without compromising viability,[56] indicating the low toxicity of DTT.

Two-photon Lithography. Based on the reactivity optimization, we finally explored 2PP thiol-ene lithography of **HA-VE**. By scanning the laser beam (Figure 10a) inside a **HA-VE**/DTT formulation with high water content (80%), a complex hydrogel construct (Figure 10b) is directly built up in 3D according to a computer-aided-design (CAD) model. After developing the sample in PBS, the gel construct was visualized by a confocal laser scanning microscope. The spatial feature size of this construct is around 4 μm, which is an intriguing size scale for a wide range of biological relevant studies. The robustness of thiol-VE reactions enabled the access to a broad processing window. Arrays of cubic structures

were screened at varying scanning speeds and laser power range. The size variance in the gel structures provides a good indication of how spatiotemporal control of photon density influences the gel crosslinking density and the resultant volumetric swelling ratio.

As shown in Figure 10c, writing speed as high as 56 mm/s was accessible, providing the feasibility of high-throughput 2PP processing of 3D hydrogel structures. Meanwhile, the formulation was processable at average laser power as low as 20 mW. At this level, laser-induced cellular damage is supposed to be negligible.[57] Together, these results lead to a conclusion that **HA-VE** gels hold great potential applications in tissue engineering and in particular for 2PP fabrication of 3D hydrogels with customized microstructures.

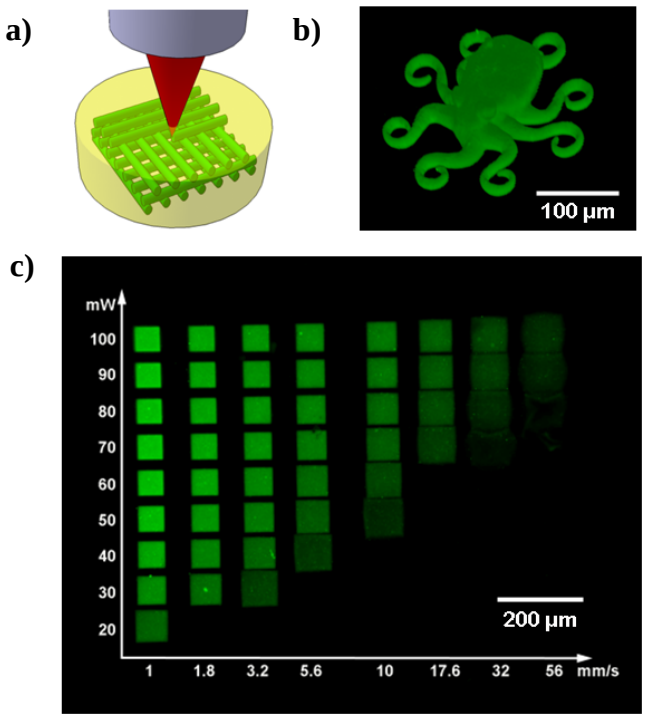

Figure 10 2PP microfabrication of a 3D hydrogel construct: **a)** schematics of the 2PP microfabrication; **b)** z-stacked laser scanning microscope image of a 3D ´´Octopus´´ construct produced by 2PP of **HA-VE**; **c)** 2PP processing window of a 10 % **HA-VE**/DTT formulation (DS=0.54, n_{-SH}:n_{-ene}=0.4).

Conclusions

In conclusion, **HA-VE**, a novel hydrogel system, was developed for high-throughput 2PP processing. **HA-VE** macromers with defined DS were successfully synthesized using lipase-catalyzed transesterification reaction. The advantages of **HA-VE** over conventional (meth)acrylated HA analogs include low cytotoxicity, PVA-based degradation products and high crosslinking efficiency when mixed with thiols. **HA-VE** hydrogels possess tunable mechanical strength that is comparable to the stiffness of varying soft tissues. Since **HA-VE** could be photopolymerized under spatiotemporal control, these injectable materials can be translated for potential (pre)clinical applications in tissue repair where photopolymerization is integrated with minimal invasive surgeries. On the other hand, we envisage that highly reactive while low cytotoxic **HA-VE** gels will further facilitate the applications of 2PP in biology and tissue engineering. These research efforts can enrich our knowledge of how mammalian cells receive information from their microenvironments in tissue development and disease. A deeper understanding of these biological activities will facilitate rational design of 3D hydrogel scaffolds with tissue-specific architectures and functions for tissue regeneration.

Experimental

Materials. All reagents were purchased from Sigma-Aldrich and used without further purification except otherwise noted.

Synthesis. *Preparation of low MW HA.* Low MW **HA** was prepared via acidic degradation of high MW HA (M_n~1.3 MDa, Fluka). High MW HA (Na^+, 5.0 g) was dissolved in distilled water to give a 0.5 wt% solution. The pH value was decreased to 1.0 by adding concentrated HCl. The degradation was performed at 60 °C under constant mechanical stirring. After 24 h, the solution was cooled down to 25 °C and the pH was increased to 7.0 by carefully adding 1 N NaOH. The resulting solution was transferred into a dialysis tubing (MW cut-off, 3.5 kDa, Carl Roth) and dialyzed against distilled water for 48 h. Finally, the solution was lyophilized, giving 3.1 g (62% of theory) of HA. Gel-permeation-chromatography (GPC) analysis showed that the number-average molar mass (M_n) of HA was 11.4 kDa with a polydispersity of 1.6.

*Preparation of tetrabutylammonium salt of HA **(HA-TBA)**.* **HA-TBA** was prepared using an protocol described by Burdick et al.[37] The sodium salt of low MW **HA** (1.0 g) was dissolved in distilled water to give a 1 wt% solution. Afterward, highly acidic ion-exchange resin (3.0 g, IR-120) was added and the resultant slurry was stirred for 4 h followed by filtration. The filtrate was neutralized to pH 7.0 by adding 20 % tetrabutylammonium hydroxide solution. This solution was directly lyophilized to give 1.54 g (99.5 % of theory) of **HA–TBA**.

*Synthesis of HA vinyl esters (**HA-VE**).* **HA-VEs** with varying DS were prepared through lipase-catalyzed transesterification. The synthesis was carried out under anhydrous conditions in order to avoid the hydrolysis of divinyl adipate (DVA, TCI). **HA-TBA** (1.0 g, 1.61 mmol) was dissolved in anhydrous DMSO to form a 1 wt% solution. Lipase acrylic resin from *Candida Antarctica B* (CAL-B, 90 mg) and hydrochinon (10 mg) was added into another flask containing either equivalent DVA (0.32 g, 1.61 mmol) or excessive DVA (0.96 g, 4.83 mmol) at 50°C. To this solution, the **HA-TBA** solution was added dropwise within 1 h. The reactions were maintained for 24 h, 48 h, 72 h, and 96h, respectively. After reaction, the mixture was diluted with distilled water by 10 times (v/v) and extracted with dichloromethane to remove excessive DVA. The extracted solution was further dialyzed against 10 mM NaCl for 24 h and later against distilled water for 48 h. After lyophilization, **HA-VE** was obtained as brown solid, giving a final yield (>80%) of starting material. The DS was determined using ^{1}H-NMR (SI, Figure S6) by comparing the integral ratio between the vinyl proton (7.20 ppm) and the N-acetyl protons (2.01 ppm). ^{1}H-NMR (D_2O): δ=7.20 (q, 1H, COC<u>H</u>=CH_2), δ=4.95 (d, 1H, COCH=C<u>H</u>$_2$), δ=4.65-4.75 (d, 1H, COC=C<u>H</u>$_2$), δ=4.55 (s, 1H, H1), δ=4.41 (s, 1H, H1′), δ=3.11-4.02 (m, 12H, H2–5, H2′–6′), δ=2.01 (s, 3H, acetyl–CH_3).

*Synthesis of HA acrylates (**HA-AC**).* **HA-AC** (DS=0.49) was prepared according to a procedure described by Novozyme.[38] Low MW HA (0.3 g, 0.75 mmol) was dissolved in distilled water (60 mL) at 5 °C. Then, drops of 0.3 N NaOH were added till reaching a pH value of 9.5. A mixture of excessive acryloyl chloride (30 eq., 22.4 mmol) and dichloromethane (60 mL) was prepared in a dropping funnel. This solution was added into the HA solution dropwise for 1 hour. During addition, pH value was maintained at 8.0-9.5 by dropwise addition of 1N NaOH. After the addition was complete, the reaction was allowed to stir for 1 hour at 5 °C. Then the reaction mixture was filtered and the filtrate was neutralized with $NaHCO_3$. Finally, the solution was dialyzed against distilled water for 24 h and lyophilized, giving 0.29 g of **HA-AC** (yield: 85% of theory). The DS of **HA-AC** was determined using ^{1}H-NMR (SI, Figure S7) by calculating the integral ratio between the acrylate protons (5.90-6.60 ppm) and the N-acetyl protons (2.01 ppm). **HA-AC** ^{1}H-NMR (D_2O): δ=5.90-6.60 (m, 3H, CH=CH_2), δ=4.55 (s, 1H, H1), δ=4.41 (s, 1H, H1′), δ=3.11-4.02 (m, 12H, H2–5, H2′–6′), δ=2.01 (s, 3H, acetyl–CH_3)

*Synthesis of HA methacrylates (**HA-MA**)* **HA-MA** (DS=0.57) was prepared by reacting **HA** with methacrylic anhydride (MA) as previously reported.[39] Low MW **HA** (0.3 g, 0.75 mmol) was firstly dissolved in distilled water (60 mL) at 5°C. MA (1.05 mL, 7.08 mmol) was added to **HA** solution dropwise under stirring. The reaction media was maintained at pH~8.5 by dropwise addition of 1 N NaOH for 3 h, followed by overnight reaction at 5 °C. The mixture was filtered and the filtrate was neutralized with $NaHCO_3$. Finally, the solution was dialyzed against distilled water (24 h). After lyophilization, 0.28 g of HA-MA was obtained as white powder in 80% yield. The DS of **HA-MA** was determined using ^{1}H-NMR (SI, Figure S8) by calculating the integral ratio between methacrylate protons (5.63, 5.31, 1.86 ppm) and the N-acetyl protons (2.01 ppm). ^{1}H-NMR (D_2O): δ=5.63 (s, 1H, C=CH_2), δ=5.31 (s, 1H, C=CH_2), δ=4.55 (s, 1H, H1), δ=4.41 (s, 1H, H1′), δ=3.11-4.02 (m, 12H, H2–5, H2′–6′), δ=2.01 (s, 3H, acetyl–CH_3), δ=1.86 (s, 3H,–CH_3).

Characterization. ^{1}H-NMR (200 MHz) spectra were measured with a Bruker ACE 2 00 FT-NMR spectrometer. The chemical shift (s = singlet, d = doublet, t = triplet, m = multiplet) is stated in ppm using the nondeuterated solvent as internal standard. Solvents with a grade of deuteration of at least 99.5% were used. GPC analysis was measured using the following system: Waters 515 HPLC pump, Waters 410 differential refractometer, Waters 486 tunable absorbance detector, and columns (7.8 mm i.d. 130 cm). The eluent was 50 mM NaCl solution/acetonitrile 80:20 (v/v), and the flow rate was 0.3 or 0.5 mL/min. The system was calibrated with standard PEG samples provided by American Polymer Standards Corporation.

Macromer Cytotoxicity. Cytotoxicities of four macromer solutions (**HA**, **HA-AC, HA-MA, HA-VE**) were evaluated via metabolic activity assay using PrestoBlue agent (Life Technologies). A mouse fibroblast cell line (L929) was cultured in high glucose Dulbecco's Modified Eagle's Medium (DMEM, Lonza) including L-glutamine, which was further supplemented with 10% fetal bovine serum and 1% penicillin-streptomycine. Macromers were dissolved in DMEM to reach final concentrations of 10% (**HA** only), 1% and 0.1%, respectively. L929 cells were seeded in a 96-well tissue culture plate at a density of 1×10^4 cells per well in 100 µL of growth medium and left to attach to the plate in the incubator (37 °C, 5% CO_2) overnight. After 24 h, the medium was removed and 100 µL of each macromer solutions were added to the cells (n=3). Cells that were not treated with the macromers were set as positive control while cells treated with DMSO were set as negative control. After 24 h incubation, macromer solutions were carefully removed and 100 µL of PrestoBlue/DMEM solution (1:10, v/v) was added. After 30 minutes of incubation at 37 °C, the fluorescence of the samples was recorded at 560 nm (excitation) and 590 nm (emission) using a microplate reader (Synergy H1, BioTek). Obtained signals were compared with fluorescence of PrestoBlue in wells without cells (blank sample – no metabolic activity of the cells), wells of negative control and wells of positive control (100 % metabolic activity).

Hydrogel Preparation. Gel precursors were dissolved in PBS solution of 0.5% Irgacure 2959 (I2959, BASF), achieving a final macromer concentration of 2.5, 5 and 10%, respectively. Hydrogel pellets were prepared in a multi-well PDMS mold (well diameter: 6 mm). Two hundred microliters of macromer solution was pipetted between two glass coverslips separated by the PDMS mold (thickness: 1.5 mm) and then exposed to UV light (20 mW/cm^2) for 900 s (450 s each side). Pellets were detached from the slides and washed twice with sterile PBS.

Photo-rheometry. A plate-to-plate time-resolved photo-rheometer (Anton-Paar MCR-301, SI, Figure S2) was used to monitor the single-photon gel formation and enzymatic degradation process of **HA-VE** gels. Filtered UV-VIS light (320-500 nm, Omnicure S2000) was directed from the bottom of the rheometer though a glass plate to the sample. Light intensity at the cure place was 10 mW·cm^{-2} as determined by an Ocean Optics USB 2000+ spectrometer. After a 60 s blank period, light was triggered to irradiate the samples. Real-time measurements were made in oscillation mode, at 25°C, 10% strain, 10 Hz and 50 µm gap thickness. Strain and frequency sweeps were performed before and post the polymerization to verify the linear response regime. The slope value of plotted G´ values (n=3) were generated from a linear regression of the G´ plots from 60 s to 200 s while the induction time was defined as the point when G´ value surpassed 5 Pa.

Enzymatic degradation of HA-VE gels was studied on the same rheometer using a procedure. adapted from Fairbanks etal.[28] Specifically, work solutions containing 10 wt% **HA-VE** (DS=0.54) and 0.5 wt% I2959 in PBS were prepared and stored on ice-bath. Varying amounts of hyaluronidase (Hase) were added into the macromer solutions giving final concentrations (10, 30, 60 mg/mL, respectively). The mixed macromer/enzyme solutions were transferred to the thermo-controlled glass plate which was set at 5 °C. Then the rheometer system adapted the solution to a 50 µm thickness. The solutions were photopolymerized *in situ* for 10 mins. Finally, the plate temperature was increased to 37 °C to activate the enzyme and initiate the enzymatic degradation.

Mass Swelling Ratio. Swelling behaviors of HA gels were tested using a generic protocol.[40] Hydrogel pellets (n=4) were prepared as aforementioned and allowed to swell in PBS for 24 h at room temperature. The wet pellets were weighed to determine the equilibrium swollen mass ($\mathbf{M_s}$) and then lyophilized to obtain the dry

weight ($\mathbf{M_d}$). The equilibrium mass swelling ratio ($\mathbf{Q_m}$) was calculated as $\mathbf{M_s/M_d}$.

AFM Modulus Test. Gel elastic moduli were analyzed using an atomic force microscopy (NanoWizard 3, JPK Instruments). Prior to test, gel samples (n=3) were UV-polymerized as aforementioned, except on top of methacrylated cover slips and then soaked in Milli-Q H_2O for 24 h. These hydrated samples were probed using a pyramidal-tipped cantilever (MSNL, Veeco Instruments). Prior to each AFM measurement, the spring constant of each cantilever was measured according to a general method,[41] with average values of 10 pN/nm. The force-indentation curves of each sample were recorded with a tip velocity of 2 µm/s and a trigger force of ~ 300 pN. Young's modulus values were calculated from the force curves according to a Hertz model (JPK software). Poisson's ratio of the gel samples was assumed as 0.5.

Two-photon Microfabrication. Gel precursor solutions were prepared as above except using a water-soluble two-photon initiator (P2CK, 2.23 mM, SI, Figure S4) which was synthesized as reported previously.[42] One hundred microliters of the precursor solution was pipetted between two glass cover slips separated by a 0.5 mm spacer. In order to fix gel structures, the bottom cover slip was pre-functionalized with methracrylate groups according to a generic protocol.[43] A Ti:sapphire laser system (HighQ Femtotrain 800 nm, 80 fs pulse duration, 75 MHz repetition rate) was used for 2PP microfabication of hydrogels. Detailed information about the 2PP experimental setup is available in a previous report of our group.[30] After 2PP processing, the sample was developed in PBS to remove unpolymerized materials. After 2 h, the gel construct was visualized by a confocal laser scanning microscope (Zeiss LSM 700).

Statistics. All error bars indicate the standard deviation. The statistical significance was determined by Student's t-Test, where '*' and '**' indicate $P<0.05$ and $P<0.01$, respectively.

Acknowledgements

Mr. Severin Mühleder (LBI-Trauma, Vienna), Dr. Jan Torgersen (TU Vienna) and Dr. Wolfgang Holnthoner (LBI-Trauma) are gratefully acknowledged for their essential role at the initial stage of this study. Dr. Zhiquan Li (TU Vienna) is particularly thanked for the synthesis of photoinitiator. Financial support from the China Scholarship Council (No 2009688014), European Research Council (Starting Grant No 307701) and European Science Foundation (P2M Network) is acknowledged.

Notes and references

[a] Institute of Applied Synthetic Chemistry, Vienna University of Technology, Getreidemarkt 6, 1060 Vienna, Austria.

[b] Institute of Materials Science and Technology, Vienna University of Technology, Favoritenstrasse 9, A-1040 Vienna, Austria.

[c] Institute of Applied Physics, Vienna University of Technology, Wiedner Hauptstrasse 8, 1040 Vienna, Austria; [+] Present Address: Lowy Cancer Research Centre, The University of New South Wales, 2052, Sydney, NSW, Australia

[a,b] Austrian Cluster for Tissue Regeneration

Corresponding Author: Prof. Dr. Robert Liska

E-mail: robert.liska@tuwien.ac.at

† Electronic Supplementary Information (ESI) available: [ATR-IR data, rheometry-setup and data (G´, G´´, gel point), cytotoxicity data of HA, chemical structure of two-photon initiator and ^{1}H-NMR spectra.]. See DOI: 10.1039/b000000x/

1 M. W. Tibbitt and K. S. Anseth, Biotechnology and Bioengineering, 2009, 103, 655-663.

2 N. Annabi, A. Tamayol, J. A. Uquillas, M. Akbari, L. E. Bertassoni, C. Cha, G. Camci-Unal, M. R. Dokmeci, N. A. Peppas and A. Khademhosseini, *Advanced Materials*, 2014, 26, 85-124.

3 O. A. Ali, P. Tayalia, D. Shvartsman, S. Lewin and D. J. Mooney, *Advanced Functional Materials*, 2013, 23, 4621-4628.

4 B. V. Slaughter, S. S. Khurshid, O. Z. Fisher, A. Khademhosseini and N. A. Peppas, *Advanced Materials*, 2009, 21, 3307-3329.

5 J. J. Rice, M. M. Martino, L. De Laporte, F. Tortelli, P. S. Briquez and J. A. Hubbell, *Advanced Healthcare Materials*, 2013, 2, 57-71.

6 C. A. DeForest and K. S. Anseth, *Annu Rev Chem Biomol Eng*, 2012, 3, 421-444.

7 S. P. Massia and J. A. Hubbell, *The Journal of Cell Biology*, 1991, 114, 1089-1100.

8 A. J. Engler, S. Sen, H. L. Sweeney and D. E. Discher, *Cell*, 2006, 126, 677-689.

9 C. S. Chen, M. Mrksich, S. Huang, G. M. Whitesides and D. E. Ingber, *Science*, 1997, 276, 1425-1428.

10 J. Malda, J. Visser, F. P. Melchels, T. Jungst, W. E. Hennink, W. J. Dhert, J. Groll and D. W. Hutmacher, *Advanced Materials*, 2013, 25, 5011-5028.

11 P. Zorlutuna, N. Annabi, G. Camci-Unal, M. Nikkhah, J. M. Cha, J. W. Nichol, A. Manbachi, H. Bae, S. Chen and A. Khademhosseini, *Advanced Materials*, 2012, 24, 1782-1804.

12 K. T. Nguyen and J. L. West, *Biomaterials*, 2002, 23, 4307-4314.

13 J. L. Ifkovits and J. A. Burdick, *Tissue Eng*, 2007, 13, 2369-2385.

14 J. Elisseeff, K. Anseth, D. Sims, W. McIntosh, M. Randolph and R. Langer, *Proceedings of the National Academy of Sciences*, 1999, 96, 3104-3107.

15 V. L. Tsang, A. A. Chen, L. M. Cho, K. D. Jadin, R. L. Sah, S. DeLong, J. L. West and S. N. Bhatia, *The FASEB Journal*, 2007, 21, 790-801.

16 B. Trappmann, J. E. Gautrot, J. T. Connelly, D. G. Strange, Y. Li, M. L. Oyen, M. A. Cohen Stuart, H. Boehm, B. Li, V. Vogel, J. P. Spatz, F. M. Watt and W. T. Huck, *Nature Materials*, 2012, 11, 642-649.

17 V. Vogel and M. Sheetz, *Nature reviews. Molecular Cell Biology*, 2006, 7, 265-275.

18 O. Guillame-Gentil, O. Semenov, A. S. Roca, T. Groth, R. Zahn, J. Voros and M. Zenobi-Wong, *Advanced Materials*, 2010, 22, 5443-5462.

19 A. Ovsianikov, V. Mironov, J. Stampfl and R. Liska, *Expert Review of Medical Devices*, 2012, DOI: 10.1586/erd.12.48, 1-21.

20 A. M. Kasko and D. Y. Wong, *Future Med Chem*, 2010, 2, 1669-1680.

21 A. M. Kloxin, A. M. Kasko, C. N. Salinas and K. S. Anseth, *Science*, 2009, 324, 59-63.

22 J. Torgersen, X.-H. Qin, Z. Li, A. Ovsianikov, R. Liska and J. Stampfl, *Advanced Functional Materials*, 2013, 23, 4542-4554.

23 C. N. LaFratta, J. T. Fourkas, T. Baldacchini and R. A. Farrer, *Angewandte Chemie*, 2007, 46, 6238-6258.

24 A. P. Zhang, X. Qu, P. Soman, K. C. Hribar, J. W. Lee, S. Chen and S. He, *Advanced Materials*, 2012, 24, 4266-4270.

25 R. Gautam, R. D. Singh, V. P. Sharma, R. Siddhartha, P. Chand and R. Kumar, *Journal of Biomedical materials research. Part B, Applied Biomaterials*, 2012, 100, 1444-1450.

26 C. Heller, M. Schwentenwein, G. Russmüller, T. Koch, D. Moser, C. Schopper, F. Varga, J. Stampfl and R. Liska, *Journal of Polymer Science Part A: Polymer Chemistry*, 2011, 49, 650-661.

27 A. Mautner, X. Qin, H. Wutzel, S. C. Ligon, B. Kapeller, D. Moser, G. Russmueller, J. Stampfl and R. Liska, *Journal of Polymer Science Part A: Polymer Chemistry*, 2013, 51, 203-212.

28 B. D. Fairbanks, M. P. Schwartz, A. E. Halevi, C. R. Nuttelman, C. N. Bowman and K. S. Anseth, *Advanced Materials*, 2009, 21, 5005-5010.

29 C. C. Lin, A. Raza and H. Shih, *Biomaterials*, 2011, 32, 9685-9695.

30 X.-H. Qin, J. Torgersen, R. Saf, S. Mühleder, N. Pucher, S. C. Ligon, W. Holnthoner, H. Redl, A. Ovsianikov, J. Stampfl and R. Liska, *Journal of Polymer Science Part A: Polymer Chemistry*, 2013, 51, 4799-4810.

31 J. A. Burdick and G. D. Prestwich, *Advanced Materials*, 2011, 23, 41-56.

32 X. Z. Shu, Y. C. Liu, Y. Luo, M. C. Roberts and G. D. Prestwich, *Biomacromolecules*, 2002, 3, 1304-1311.

33 D. A. Ossipov, X. Yang, O. Varghese, S. Kootala and J. Hilborn, *Chem Commun*, 2010, 46, 8368-8370.

34 C. M. Nimmo, S. C. Owen and M. S. Shoichet, *Biomacromolecules*, 2011, 12, 824-830.

35 J. Baier Leach, K. A. Bivens, C. W. Patrick, Jr. and C. E. Schmidt, *Biotechnology and Bioengineering*, 2003, 82, 578-589.

36 X. Jia, J. A. Burdick, J. Kobler, R. J. Clifton, J. J. Rosowski, S. M. Zeitels and R. Langer, *Macromolecules*, 2004, 37, 3239-3248.

37 S. Khetan, J. S. Katz and J. A. Burdick, *Soft Matter*, 2009, 5, 1601-1606.

38 WO2007106738A2, 2007.

39 S. Khetan, M. Guvendiren, W. R. Legant, D. M. Cohen, C. S. Chen and J. A. Burdick, *Nature Materials*, 2013, 12, 458-465.

40 J. W. Nichol, S. T. Koshy, H. Bae, C. M. Hwang, S. Yamanlar and A. Khademhosseini, *Biomaterials*, 2010, 31, 5536-5544.

41 J. L. Hutter and J. Bechhoefer, *Rev Sci Instrum*, 1993, 64, 1868-1873.

42 Z. Li, J. Torgersen, A. Ajami, S. Muhleder, X. Qin, W. Husinsky, W. Holnthoner, A. Ovsianikov, J. Stampfl and R. Liska, *RSC Advances*, 2013, 3, 15939-15946.

43 C. A. Goss, D. H. Charych and M. Majda, *Anal Chem*, 1991, 63, 85-88.

44 A. Kowitsch, Y. Yang, N. Ma, J. Kuntsche, K. Mader and T. Groth, *Biotechnology and Applied Biochemistry*, 2011, 58, 376-389.

45 H. Uyama and S. Kobayashi, *Enzyme-Catalyzed Synthesis of Polymers*, 2006, 194, 133-158.

46 N. Wang, Z. C. Chen, D. S. Lu and X. F. Lin, *Bioorg Med Chem Lett*, 2005, 15, 4064-4067.

47 J. Yeh, Y. Ling, J. M. Karp, J. Gantz, A. Chandawarkar, G. Eng, J. Blumling Iii, R. Langer and A. Khademhosseini, *Biomaterials*, 2006, 27, 5391-5398.

48 S. J. Bryant, C. R. Nuttelman and K. S. Anseth, *Journal of Biomaterials Science. Polymer Edition*, 2000, 11, 439-457.

49 A. M. Kloxin, C. J. Kloxin, C. N. Bowman and K. S. Anseth, *Advanced Materials*, 2010, 22, 3484-3494.

50 D. E. Discher, P. Janmey and Y. L. Wang, *Science*, 2005, 310, 1139-1143.

51 G. L. Kennedy, Jr., *Drug and Chemical Toxicology*, 2002, 25, 191-202.

52 A. Takahashi, Y. Suzuki, T. Suhara, K. Omichi, A. Shimizu, K. Hasegawa, N. Kokudo, S. Ohta and T. Ito, *Biomacromolecules*, 2013, 14, 3581-3588.

53 I. Schoen, B. L. Pruitt and V. Vogel, *Annual Review of Materials Research*, 2013, 43, 589-618.

54 C. E. Hoyle and C. N. Bowman, *Angewandte Chemie*, 2010, 49, 1540-1573.

55 K. D. Held and D. C. Melder, *Radiation Research*, 1987, 112, 544-554.

56 C. S. Ki, H. Shih and C. C. Lin, *Biomacromolecules*, 2013, 14, 3017-3026.

57 A. Ovsianikov, S. Muhleder, J. Torgersen, Z. Li, X. H. Qin, S. Van Vlierberghe, P. Dubruel, W. Holnthoner, H. Redl, R. Liska and J. Stampfl, *Langmuir*, 2014, 30, 3787-3794.1.

